Molecular Biotechnology (2020) 62:132–141
https://doi.org/10.1007/s12033-019-00231-0

ORIGINAL PAPER

Molecular Cloning, Characterisation, and Heterologous Expression of Farnesyl Diphosphate Synthase from *Sanghuangporus baumii*

Xutong Wang[1] · Tingting Sun[2] · Jian Sun[1] · Shixin Wang[1] · Yisha Ma[1] · Zengcai Liu[1] · Jian Zhang[1] · Guoquan Zhang[1] · Li Zou[1]

Published online: 2 January 2020

Abstract

A farnesyl diphosphate synthase (*FPS*) cDNA and promoter region was cloned from *Sanghuangporus baumii*. The gene contains a 150-bp 5′-untranslated region (UTR), a 154-bp 3′-UTR, and a 1062-bp open reading frame (ORF) encoding a 354 amino acid polypeptide. The *FPS*-DNA includes three exons (nucleotides 1 –123, 184–321, and 505–1305) and two introns (nucleotides 124–183 and 322–504). The FPS protein has a molecular weight of 40.73 kDa, it is hydrophilic with a theoretical isoelectric point of 5.13, and the secondary and three-dimensional structure were analysed. There is a transcription start site at nucleotides 1318–1368 of the promoter, which includes typical eukaryotic promoter elements (TATA Box, CAAT Box, ARBE, AT-rich element, G-box, MBS, Sp1, LTR). *FPS* was expressed in *Escherichia coli* BL21, and the recombinant protein (63.41 kDa) was subjected to dodecyl sulphate, sodium salt-polyacrylamide gel electrophoresis (SDS-PAGE). *FPS* transcription was measured during different developmental stages, and expression in 11 and 13 days mycelia was upregulated 49.3-fold and 125.4-fold, respectively, compared with 9 days mycelia controls. Through analysing, *S. baumii* triterpenoid content was correlated with the transcription level of *FPS* during different development stages, and the triterpenoid content peaked at day 15 (7.21 mg/g).

Keywords *Sanghuangporus baumii* · Farnesyl diphosphate synthase · Triterpenoids · Promoter · Intron analysis · Quantitative real-time PCR · Recombinant expression · Bioinformatics

Introduction

Sanghuangporus baumii, a precious medicinal fungus, is considered one of the most effective anticancer fungi. *S. baumii* was placed in the genus *Inonotus* (*Inonotus baumii*), but it is now in the genus *Sanghuangporus* [1]. This species possesses significant anti-tumour [2, 3], anti-oxidation [4], anti-inflammatory [5], anti-ageing [6], blood sugar-lowering [7], and immunity enhancement [8] activities. Furthermore, *S. baumii* can generate various secondary metabolites such as polysaccharides, ergosterol, and triterpenoids [9, 10].

✉ Li Zou
372138603@qq.com

[1] College of Forestry, Northeast Forestry University, Hexing Road 26, Xiangfang District, Harbin 150040, Heilongjiang, China

[2] Department of Food Engineering, Harbin University, Zhongxing Road 109, Nangang District, Harbin 150086, Heilongjiang, China

Triterpenoids are important for *S. baumii* development, and these medicinal active ingredients can improve human immunity and exert anti-tumour effects. Previous research on *S. baumii* triterpenoids has mainly focussed on separation and measurement methods [11–13], but the synthetic mechanism has not been reported. There are relatively few examples of using triterpenoids for medical treatment, largely due to low production yield.

Farnesyl diphosphate synthase (FPS) catalyses the condensation of dimethylallyl diphosphate (DMAPP) with two units of isopentenyl pyrophosphate (IPP) to produce farnesyl pyrophosphate (FPP), a key intermediate located at the branch point in the mevalonate (MVA) pathway and precursor of several terpenes including sesquiterpenes, sterols, and triterpenes [14]. Triterpenes are synthesised via two pathways (Fig. 1): the MVA pathway and the non-mevalonate pathway through 2C-methyl-D-erythritol-4-phosphate (MEP) or 1-deoxy-D-xylulose-5-phosphate (DOXP) [15]. The MVA pathway is dominant in most eukaryotes, a few archaea, and fungi [15], and it provides precursors for algae,

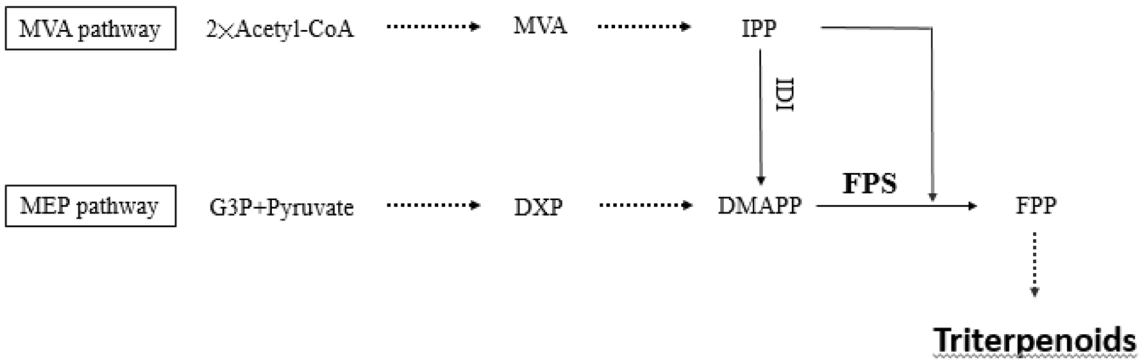

Fig. 1 The triterpenoid biosynthetic pathway of *S. baumii*. *MVA* mevalonate, *IPP* isopentenyl diphosphate, *G3P* glyceraldehyde-3-phosphate, *DXP* 1-deoxy-D-xylulose-5-phosphate, *DMAPP* dimethylallyl diphosphate, *IDI* diphosphate isomerase

cyanobacteria, and plants [16]. Two molecules of acetyl-CoA are converted to IPP through various chemical reactions in the MVA pathway, and the biosynthesis of FPP is subsequently catalysed by FPS to generate terpenoids [17, 18] (Fig. 1).

FPS catalyses the synthesis of FPP that serves as a precursor for various products including terpenoids, lanosterol, and dolichols [19]. FPS is located at the first branch of the isoprenoid biosynthesis pathway, and manipulation of this enzyme can alter the yield of downstream products in prokaryotes and eukaryotes [20]. For example, *FPS* from *Gossypium arboreum* is placed under the control of the CaMV35S promoter, plant expression vectors were transferred into *Artemisia annua* via *Agrobacterium tumefaciens* LBA4404, and the yield of transgenic *A. annua* artemisinin (3.01 mg/g) was 3–4-fold higher than that of the wild-type plant, demonstrating the *FPS* plays an important role in biosynthesis in this species [21].

FPS not only affects the yield of secondary metabolite, but also regulates transcription levels of downstream genes and enhances metabolic flux of triterpenoids. Homologous *FPS* is transferred in *Panax japonicas*, and the expressions of other key enzyme genes are promoted because the metabolic flux of saponins is increased [22]. Overexpression of the *FPS* upregulates the transcription levels of SQS and LS genes and increased production of Ganoderic acids in *Ganoderma lucidum* [23]. Overexpression of the *Centella asiatica FPS* gene in *Panax giseng* shows that no differences are detected in any expression of all genes, but the content of total ginsenosides is increased than that of the controls [24]. *FPS* from *S. baumii* is of significant interest but it has not yet been fully characterised. Thus, investigating *FPS* expression and its association with triterpenoid production during different developmental stages is a research priority. Expression levels of *Withania somnifera FPS* were found to be highest in flowers and young leaves [25], and expression of *G. lucidum GlFPS* in the primordia is 53.9-fold higher than in the mycelia, suggesting that *GlFPS* transcription is regulated during different developmental stages [26].

In the present study, a farnesyl diphosphate synthase cDNA and promoter region from *S. baumii* were cloned and characterised, and recombinant protein was produced in *Escherichia coli* BL21 (DE3). *FPS* transcription and triterpenoid content was explored during different developmental stages.

Materials and Methods

Strain and Plasmids

Sanghuangporus baumii was obtained from Xiaoxing Anling in Yichun City, Heilongjiang Province, China, and authenticated by internal transcribed spacer (ITS) sequence alignment. The pMD18-T vector (TaKaRa, Beijing, China) and the pET-32a(+) vector were used as cloning and expression vectors. *E. coli* DH5α and BL21 (DE3) strains (Tiangen, Beijing, China) were used to construct and express recombinant vectors, and cells were grown in Luria–Bertani (LB) broth. *S. baumii* was inoculated on potato dextrose agar (PDA) medium, incubated without light at 26 °C for 9 days, placed in liquid PD medium, and cultured in a constant temperature shaking incubator at 26 °C and 180 rpm.

RNA and cDNA Extraction

Mycelia from *S. baumii* were cultured for 9 days in PD medium, and mycelia were collected with a sterile gauze and frozen at − 80 °C. *S. baumii* total RNA was purified using a Plant Total RNA Extraction Kit (Tiangen) according to the manufacturer's instructions. *S. baumii* cDNA was amplified using a PrimeScript first-strand cDNA synthesis kit (TaKaRa).

Amplification of a Specific Fragment of FPS

The *FPS* sequence was obtained from the *S. baumii* transcriptome database. Using gene annotation and BLAST, 12 candidate unigenes were identified in the MVA pathway, and we found an *FPS* gene fragment (Unigene26476) [26]. *FPS*-f1 and *FPS*-r1 primers were generated based on the *FPS* sequence and used to amplify the *FPS*-cDNA fragment (Table 1 Reactions (50 µL) contained 25 µL of Premix Taq, 19 µL of ddH_2O, 2 µL of FPS-f1, 2 µL of FPS-r1, and 2 µL of *S. baumii* cDNA. Thermal cycling was performed at 94 °C 5 min, followed by 35 cycles at 94 °C for 30 s, 57 °C for 30 s, 72 °C for 40 s, and a final extension at 72 °C for 10 min. The DNA fragment was purified and ligated into the pMD18-T vector, and the resulting construct was transformed into of *E. coli* DH5α strain for nucleotide sequencing (Boshi, Harbin, China).

RACE-PCR and Amplification the Full Length of the *FPS*-cDNA

The 3′ and 5′ cDNAs were extracted using a SMARTer RACE-cDNA amplification kit (Clontech, San Francisco, USA) according to the specifications. Based on the *FPS*-cDNA fragment sequence, homologous primers (*FPS*-3-1 and *FPS*-5-1) were designed (Table 1). Using an Advantage 2 PCR kit (Clontech), the 3′ and 5′ ends of *FPS* were cloned using the RACE-PCR technique in a 50 µL containing 34.5 µL of PCR-grade water, 5 µL of 10 × Advantage 2 PCR Buffer, 1 µL of dNTP Mix (10 mM), 1 µL of 50 × Advantage 2 Polymerase Mix, 2.5 µL of 3′ RACE-cDNA or 5′ RACE-cDNA, 5 µL of UPM (10 ×), and 1 µL of FPS-3-1 or FPS-5-1. The 3′ and 5′ RACE-PCR program consisted of an initial denaturation step at 94 °C for 3 min, followed by 35 cycles at 94 °C for 30 s, 68 °C for 30 s, 72 °C for 40 s, and a final extension at 72 °C for 7 min. The 3′ and 5′ fragments were inserted into the pMD18-T vector, and the resulting construct was transformed into *E. coli* DH5a competent cells [13].

Next, the entire *FPS*-cDNA was deduced by aligning and splicing the nucleotide sequences of the 3′ and 5′ RACE products. Using *S. baumii* cDNA as template, the whole *FPS*-cDNA was cloned with Premix Taq (EX Taq Version 2.0 plus dye; TaKaRa) and primers *FPS*-f-*Bam*HI (based on the cDNA sequence from nucleotides 1–31, and containing an ATG start codon and *Bam*HI restriction enzyme cutting site) and *FPS*-r-*Hind*III (complementary to the DNA sequence from 1038 to 1071 and containing a TGA stop codon and *Hind*III restriction enzyme cutting site). Amplification reactions (50 µL) contained 25 µL of Premix Taq, 19 µL of DEPC, 2 µL of FPS-f-BamHI, 2 µL of FPS-r-HindIII, and 2 µL of *S. baumii* cDNA. Thermal cycling involved an initial denaturation step at 94 °C for 5 min, followed by 35 cycles at 94 °C for 30 s, 61 °C for 30 s, 72 °C for 40 s, and a final extension at 72 °C for 7 min. The product was purified using a MiniBEST DNA Fragment Purification Kit Ver.4.0 (TaKaRa), cloned into the pMD18-T vector (pMD18-*FPS*), and the resulting construct was transformed into *E. coli* DH5α. Positive single colonies were selected and incubated in LB medium in a constant temperature shaking incubator (37 °C, 180 rpm, 7 h). The resulting plasmid was sequenced by Boshi company (Harbin, China).

Amplification of the *FPS*-DNA and Promoter

FPS-DNA was amplified from *S. baumii* mycelia using the cetyltrimethylammonium ammonium bromide (CTAB)

Table 1 Primers used for PCR amplification

Primers	Sequences (5′- 3′)	Descriptions
FPS-f1	CACAGATGTCACCTCGTCCCCAACG	For *FPS*-cDNA fragment sequence amplification
FPS-r1	GTTTCATGCATGAGGTCTAACAGG	
FPS-3-1	TCTCCAAGAGCCATGTCAAGCAAAC	For RACE
FPS-5-1	TACACTCCAGCCAAGAATTGCCGC	
FPS-f-*Bam*HI	CGCGGATCCATGTCAAGCAAACAGGACAAGC	For full-length *FPS*-cDNA isolation
FPS-r-*Hind*III	CCCAAGCTTTCACTTCGTGCGCTTATAGATCTT	
FPS-DNA-f	ATGTCAAGCAAACAGGACAAGC	For full-length *FPS*-DNA isolation
FPS-DNA-r	TCACTTCGTGCGCTTATAGATCTT	
FPS-RT-f	CCGTGGCATTTCCGTAACAGAC	For qRT-PCR analysis
FPS-RT-r	CAGCAGGGTTGTCCTCTCCGTGT	
β-tubulin-f	GCTGAATATCGTTCGTGCCC	For qRT-PCR analysis
β-tubulin-r	ATCCGCCTTCCTCCTTACAGT	
FPS-Pro-f	CGGAGTCGTTGGATTCTTCAGTGTA	For *FPS* promoter isolation
FPS-Pro-r	TCGCAAGATATTCGATCAGCTCATC	

method. The entire *FPS*-DNA was obtained by PCR amplification with primers *FPS*-DNA-f and *FPS*-DNA-r (Table 1). *FPS* promoter primers (*FPS*-Pro-f and *FPS*-Pro-r; Table 1) were designed based on *S. baumii* genomic DNA. Thermal cycling involved an initial denaturation step at 94 °C for 5 min, followed by 35 cycles at 94 °C for 30 s, 60 °C for 30 s, 72 °C for 40 s, and a final extension at 72 °C for 7 min. The resulting fragment was transformed into the pMD18-T vector and sequenced by Boshi company.

Sequence Analysis

The *FPS*-cDNA and DNA were compared to verify the size and location of exons and introns. Subsequently, the FPS sequence was obtained using ORF Finder (https://www.ncbi.nlm.nih.gov/orffinder/), and the *FPS* sequence was compared using the NCBI database (https://blast.ncbi.nlm.nih.gov/Blast.cgi?PROGRAM=blastx&PAGE_TYPE=BlastSearch&LINK_LOC=blasthome). Evolutionary trees were constructed using the neighbour-joining method in the MEGA 6.0 program, and FPS sequences from other species were acquired from NCBI.

The molecular weight, amino acid composition, theoretical isoelectric point (pI), and hydrophilicity of the protein were predicted by ProtParam software (https://web.expasy.org/protparam/). The transmembrane region was identified by TMHMM Sever v.2.0 (https://www.cbs.dtu.dk/services/TMHMM/). Protein structural and signal peptide prediction were conducted with the SMART tool (https://docs.citrix.com/en-us/smart-tools) and SignalP 4.0 Server software (https://www.cbs.dtu.dk/services/SignalP/), respectively. The secondary structure of FPS was determined by the predictant protein tool (https://www.predictprotein.ong/). The three-dimensional structure of FPP was modelled by SWISS-MODEL (https://www.swissmodel.expasy.org/interactive). The transcription start site was predicted using the Berkeley Drosophila Genome Project tool (https://www.fruitfly.org/seq_tools/promoter.html). The *FPS* promoter was analysed using PlantCARE (https://bioinformatics.psb.ugent.be/webtools/plantcare/html/).

Heterologous Expression of *FPS* in *E. coli*

The pMD18-*FPS* plasmids were extracted using a Plasmid Mini kit I (OMEGA, Georgia, USA). Amplification products were double-digested with restriction enzymes (QuickCut *Bam*HI and *Hind*III; TaKaRa) and inserted into the linearised pET-32a(+) vector (pET-*FPS*) using T4 DNA Ligase (TaKaRa). The resulting pET-*FPS* plasmids were transferred into *E. coli* DH5α and *E. coli* BL21 (DE3). *E. coli* BL21 cells containing the pET-*FPS* plasmids were confirmed by PCR and double digestion. *E. coli* BL21 cells containing pET-FPS plasmids were inoculated into 50 mL LB liquid medium and incubated in a 37 °C constant temperature incubator (200 rpm) to an optical density at 600 nm (OD600) of 0.5–0.8, and 1 mL of bacterial solution was taken out as a negative control. *E. coli* BL21 cells containing only the pET-32a(+) vector were also used as controls. Protein expression was induced with 1 mM isopropyl b-D-1-thiogalactopyranoside (IPTG) and culturing was continued at 28 °C with shaking at 200 rpm. A 1 mL sample of bacterial solution was collected every 2 h until 10 h, centrifuged at 10,000 rpm for 10 min, and cells were resuspended in 100 µL of 4× dodecyl sulphate, sodium salt-polyacrylamide gel electrophoresis (SDS-PAGE) loading buffer (Solarbio, Beijing, China) with dithiothreitol (DTT) and incubated in boiling water for 10 min. Proteins (8 µL) were separated using a TRIS-Tricine-SDS-PAGE kit (Solarbio) and compared with a 10 µL sample of 14.4–97.4 kD Protein Markers (Solarbio). The voltage for electrophoresis was 80 V initially, then 120 V when the sample reached the separating gel. The gel was soaked in Coomassie Brilliant Blue Fast Staining solution (Solarbio) for 4–5 h and then placed in decolourising solution.

Transcription Analysis of *FPS* in *S. baumii*

Total RNA from mycelia, primordia, and young fruiting bodies was extracted using an RNAprep pure PlantKit (Tiangen) according to the manufacturer's instructions, and first-strand cDNA was produced using a PrimeScript RT Reagent Kit with gDNA Eraser (Takara). Subsequently, quantitative real-time PCR (qRT-PCR) was performed using SYBR Green-Master Mix (Takara) on an Mx3000P Sequence Detection System (Agilent Technologies, California, USA). Reactions (20 µL) contained 1 µL of cDNA template, 0.4 µL of Forward Primer (10 µM), 0.4 µL of Reverse Primer (10 µM), 10 µL of 2× Real Star Green Power Mixture, and 8.2 µL of ddH_2O. Primers were designed for qRT-PCR (Table 1), and thermal cycling involved an initial denaturation step at 95 °C for 3 min, followed by 40 cycles at 95 °C for 30 s, 57 °C for 30 s, 72 °C for 1 min, and a final extension at 72 °C for 10 min. Each sample was repeated in triplicate. Mycelia from day 9 served as a control sample, and β-tubulin was used as an internal reference gene. Transcription levels were calculated using the $2^{-\Delta\Delta C_t}$ method [27]. Statistical analysis

was performed using analysis of variance (ANOVO), and a *p*-value of 0.05 was considered statistically significant.

Measuring *S. baumii* Triterpenoids

In order to explore the relationship between *FPS* transcription level and triterpenoids, the *S. baumii* triterpenoid content was measured in mycelia, primordia, and young fruiting bodies. *S. baumii* triterpenoids contain ursolic acid [28]. Therefore, a standard curve was generated using ursolic acid (Shanghai Yuanye Bio-technology company, Shanghai, China) [29]. Determination of *S. baumii* triterpenoids was performed as described previously [11]. *S. baumii* mycelia, primordia, and young fruiting bodies were pulverised using a pulveriser (Taisite, Tianjin, China). *S. baumii* powder was sifted using a sifter (aperture 0.25 mm; Jiangshan, China), dissolved in 70% ethyl alcohol at 500 mg/mL and then placed in a KQ ultrasonic cleaning machine (Kunshan Ultrasonic Instruments, Kunshan, China) for 40 min at 60 °C and 100 W (40 kHz). Extracts were filtered through a qualitative filter paper (15–20 μm) (Hangzhou Fuyang Wood Pulp Paper Company, Hangzhou, China). A 50 μL sample of filtered extract was placed in a centrifuge tube and dried at 70 °C in a thermostatic water bath (Senxin, Shanghai, China). Residues were resuspended in 4 mL 5% vanillin-acetic acid and 1 mL perchloric acid, incubated at 60 °C for 20 min, and cooled rapidly. Subsequently, 5 mL glacial acetic acid was added and incubated at 25 °C for 15 min. The absorbance at 548 nm was measured using a spectrophotometer (Youke, Shanghai, China), and absorbance data were used to calculate triterpenoids content according to the standard curve.

Results

Sequence Analysis of the *FPS*

A 626-bp *FPS* fragment was identified in the *S. baumii* transcriptome data, and this gene fragment was similar to other *FPS* fragments in the NCBI database. The 5′ and 3′ cDNA ends were determined using electronic splicing, an a 1375-bp *S. baumii FPS* sequence was obtained that includes a 5′-untranslated region (UTR) of 159 bp, a 3′-UTR (154 bp), and an open reading frame (ORF) of 1062-bp encoding a 354 amino acid polypeptide. Comparison of the nucleotide sequence of the *FPS*-DNA (1305 bp) with that of the *FPS*-cDNA revealed that the gene contains three exons (nucleotides 1–123, 184–319, and 503–1303) and two introns (124–183 bp and 320–502 bp; Fig. 2).

Analysis of the Deduced Protein Sequence

The *FPS* cDNA sequence had be deposited in the GenBankdata base (GenBank accession number: MN006823) and shares highest sequence similarity and query coverage with its homolog in *Schizopora paradoxa* (71% and 100%, respectively). The *S. baumii* FPS sequence was BLAST searched against the NCBI database, and 27 homologous protein sequences were used for phylogenetic tree construction (Fig. 3), which showed that FPS from *S. baumii* is most similar to *FPS* from *Schizopora paradoxa*, but more distantly related to *Rhodotorula toruloides FPS* and *Tremella mesenterica FPS*. Using the ProtParam tool, the molecular weight of FPS is predicted to be 40.73 kDa, the theoretical pI is 5.13, and there are 54 negatively charged amino acid residues (Asp + Glu) and 42 positively charged amino acid residues (Arg + Lys). Leucine (Leu) accounted for the highest proportion (11%), and tryptophan (Trp) accounted for the lowest proportion (1.1%) in the amino acid sequence.

The protein instability index is 45.18, indicating that FPS is unstable according to the Guruprasad K method [27]. Hydrophobicity (2.14) is highest for the 200–250 amino acid region, and hydrophilicity (− 2.51) is highest for the 0–50 amino acid region. There are more hydrophilic than hydrophobic amino acids, suggesting that the protein is hydrophilic overall.

Analysis of FPS using the TMHMM Server (v.2.0) demonstrated that amino acids 1 to 187 are located at the cell membrane surface, and residues 108 to 210 form a typical transmembrane helix region. A signal peptide does not appear to

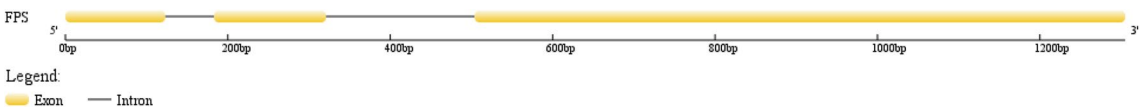

Fig. 2 Exons and introns in *S. baumii FPS*

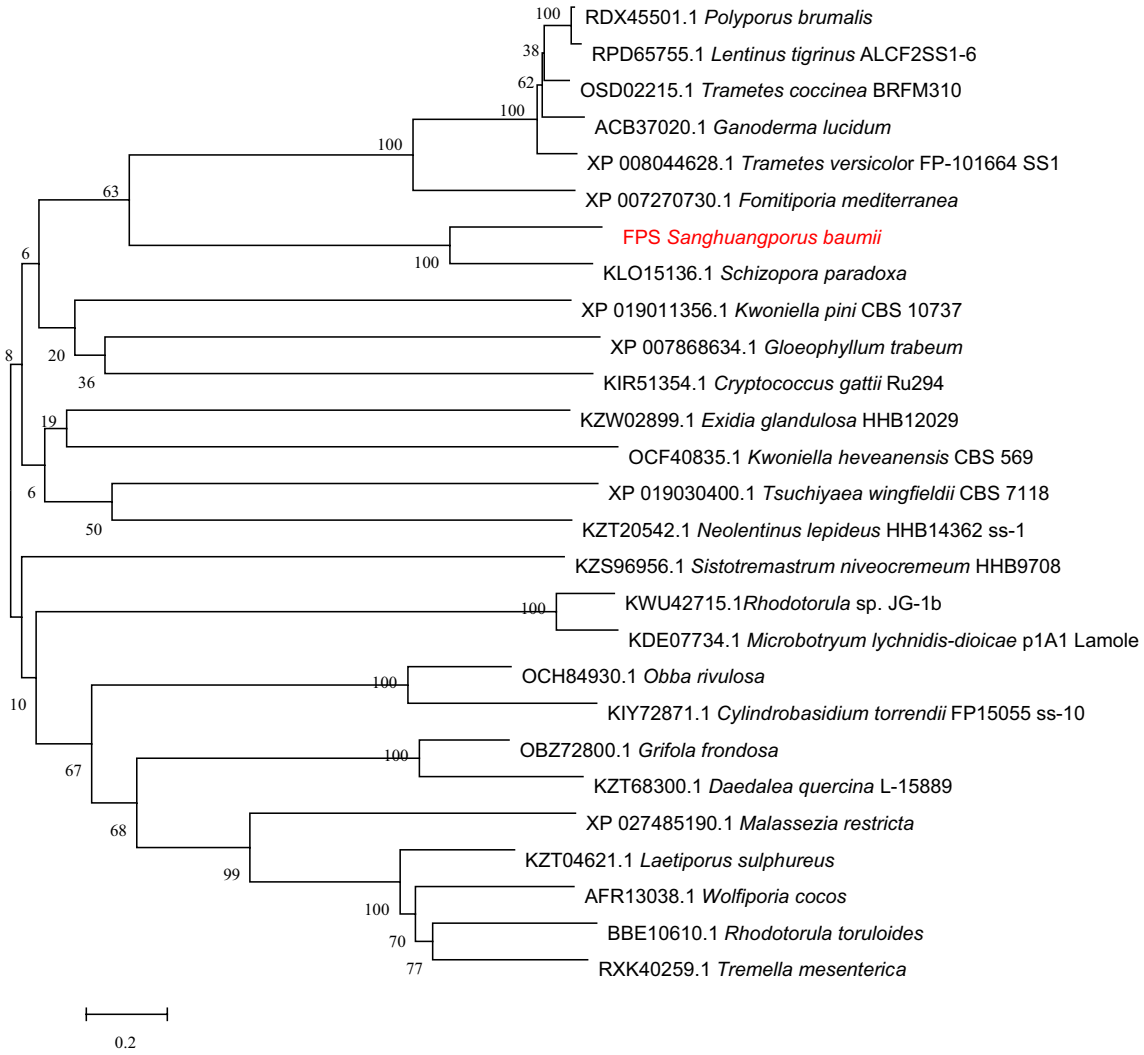

Fig. 3 Phylogenetic tree of FPS protein sequences of various species

be present. Analysis of structural functional domains revealed highly a conserved structural domain spanning resides 41 to 311, and secondary structural prediction indicates 44.76% α-helix, 11.61% β-sheet, and 43.63% random coil [29]. Three-dimensional structure prediction was performed based on the X-ray and a homologous protein sharing 49.12% sequence similarity with *S. baumii* FPS [30-36] (Fig. 4).

Analysis of the *FPS* Promoter

The 1754-bp *FPS* promoter contains a 50-bp *FPS*-cDNA spanning nucleotides 1318–1368 (GenBank accession number MN006823). The *FPS* promoter contains typical eukaryotic promoter elements, including 16 TATA boxes (with a core promoter element 30-bp upstream of the transcription start site), 17 CAAT boxes (common *cis*-acting element in promoter and enhancer regions), an ARBE sequence

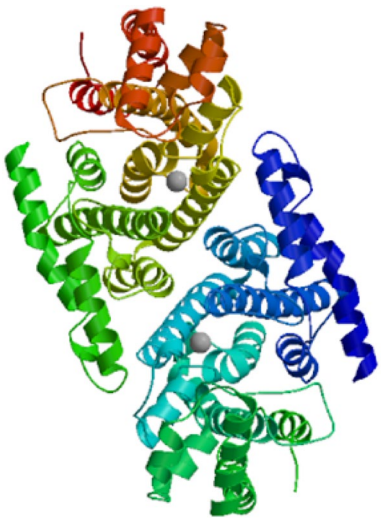

Fig. 4 Three-dimensional structure prediction and schematic representation of the *S. baumii* FPS protein

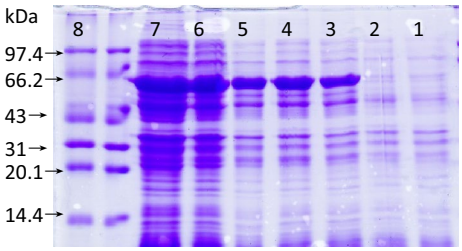

Fig. 5 Heterologous expression of *S. baumii FPS* in *E. coli* via IPTG induction (1 mM) at 37 °C for 0, 2, 4, 6, 8, and 10 h. Lane 1, *E. coli* harbouring empty vector; Lane 2–7, *E. coli* harbouring the pET-32a-abf construct induced by IPTG (1 mM) for 0, 2, 4, 6, 8, and 10 h; Lane 8, protein markers (14.4–97.4 kDa)

(*cis*-acting element involved in abscisic acid responsiveness), two G-boxes (*cis*-acting regulatory element involved in light responsiveness), an AT-rich element (binding site for AT-rich DNA-binding proteins), an Sp1 motif (light-responsive element), an MBS sequence (MYB-binding site involved in drought inducibility), and an LTR motif (*cis*-acting element mediating low-temperature responsiveness).

Expression of Recombinant FPS

Escherichia coli BL21 cells containing pET-*FPS* plasmids were induced by IPTG for 2, 4, 6, 8, and 10 h in order to test *FPS* expression. The expected protein bands (40.73 kDa + 22.68 kDa tag protein) were identified in SDS-PAGE analysis (Fig. 5). The FPS protease yield was not correlated with induction time.

Transcription of *FPS* During Different Development Stages

Sanghuangporus baumii FPS was expressed in all six developmental stages tested, and differences between stages were significant (Fig. 6). *FPS* transcription increased continuously over time and reached a relatively high level on day 13 in mycelia. The transcription level then decreased gradually thereafter. Transcription of *FPS* in mycelia after 11 and 13 days was upregulated 49.3-fold and 125.4-fold, respectively, and upregulation was significant after only 9 days, compared with controls. *FPS* transcription levels in *FPS* primordia and young fruiting bodies were approximately 8.5-fold and 6.3-fold higher than controls, respectively. FPS is placed at the branch point in the isoprenoid biosynthesis pathway and is a crucial enzyme in isoprenoid biosynthesis [14]. Thus, its transcription can have a dramatic effect on the production of triterpenoids.

Sanghuangporus baumii Triterpenoid Content During Different Development stages

The triterpenoid content in *S. baumii* mycelia was found to differ significantly between different developmental stages (Fig. 7). It gradually increased from day 9 and peaked at day 15 (7.21 mg/g) and then decreased to 5.02 mg/g. Meanwhile, triterpenoid levels in young fruiting bodies reached 6.26 mg/g.

Discussion

Sanghuangporus baumii strains frequently produce low levels of triterpenoids, which is a barrier to their use in medical treatments. Therefore, modifying strains through molecular biology-based and genetic engineering strategies to enhance metabolite yield is a research priority. Triterpenoids from *S. baumii* are useful medicinal ingredients, but the genes encoding enzymes responsible for the isoprenoid biosynthesis pathway are poorly characterised. In the present

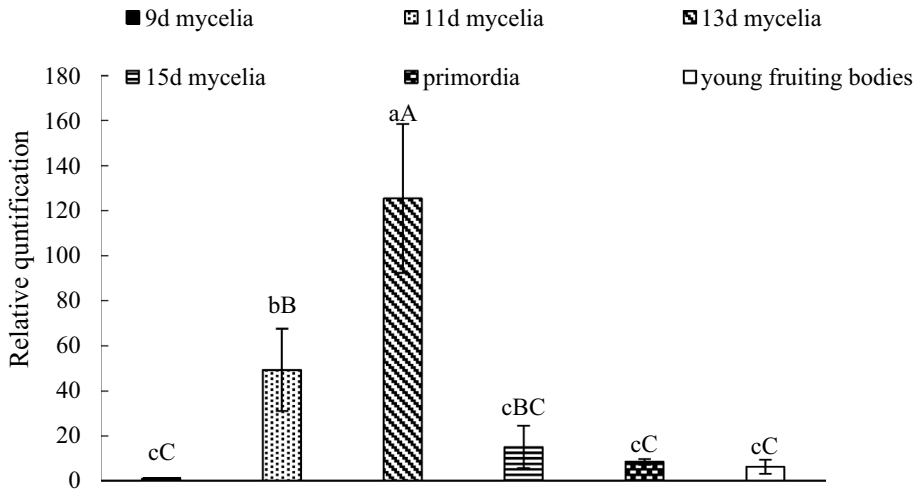

Fig. 6 Expression level of the *FPS* gene in *S. baumii* during different developmental stages

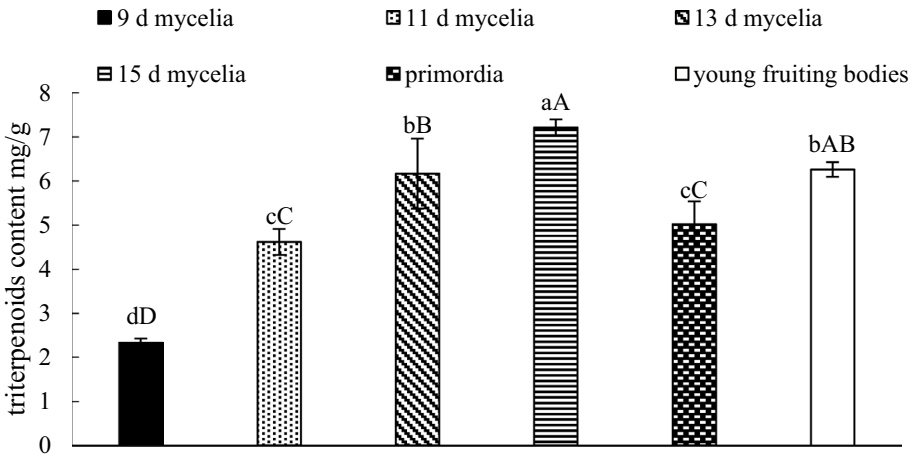

Fig. 7 *Sanghuangporus baumii* triterpenoid content during different developmental stages

study, the *S. baumii FPS* sequence was cloned for the first time using RACE technology. The sequence was analysed by bioinformatics software, and the results indicated 71% similarity between *S. baumii* and *S. paradoxa* homologs. The *S. baumii* FPS has a molecular weight of 40.73 kDa and it is hydrophilic. The 1305-bp *FPS*-DNA contains three exons and two introns. The size of the *FPS* gene in archaea (*Aeropyrum pernix*) [37], yeast (*Saccharomyces cerevisiae*) [38], fungi (*Ganoderma lucidum*) [26], and plants (*Artemisia tridentata* and *Maize*) [39, 40] ranges from 1 to 2.1 kb. Plant (Arabidopsis and apple) *FPS* genes contain 11–12 exons, but fungi contain four exons. Available information of fungal *FPS* is limited; hence, studies on *FPS* exons and introns should be helpful for future work on protein expression and triterpenoid biosynthesis.

The *S. baumii FPS* promoter contains typical fungal promoter elements and shares some similarities with the *G. Lucidum FPS* promoter, including a TATA box, a CAAT box, an ARBE motif, a G-box, an MBS sequence, and Sp1 and LTR motifs [41]. Research on the *FPS* promoter sequence may be favourable for understanding gene functions in triterpenoid biosynthesis and may provide general insight into the triterpenoid biosynthesis pathway.

In addition, transcription of *FPS* in *S. baumii* was investigated during different development stages. On day 13 of mycelia fermentation, transcription levels of *FPS* were higher than in primordia and young fruiting bodies. In past studies, transcription levels of *G. Lucidum FPS* were found to be highest in primordia [41]. *S. baumii* might therefore produce a larger quantity of triterpenoids during the mycelial growth stage. Zhang [11] showed that the content of triterpenoids in *Inonotus baumii* mycelia is higher than in fruiting bodies, which is consistent with our current results.

In order to investigate *FPS* function and regulation, the *S. baumii* triterpenoid content was measured, and this peaked in mycelia after 15 days. The triterpenoid content in primordia initially decreased, albeit the transcription level began to decrease in mycelia after 15 days. The triterpenoids content enhanced again in young fruiting bodies, but the transcription level did not increase significantly. This could be because gene expression is dependent on a series of reactions and processes, including protein dimerisation, protein, and gene binding interactions, transcription, and translation. Protein dimerisation and gene binding interactions are generally rapid. However, transcription and translation are slow and involve multiple complex steps, potentially leading to a pronounced lag phase. Therefore, *S. baumii* triterpenoid content was correlated with the transcription level of *FPS* during different development stages, as described previously [42]. After expression of *FPS* was upregulated, the triterpenoid content was also upregulated. Additionally, FPS is not only responsible for the synthesis of the precursor of *S. baumii* triterpenoids, but also cholesterol and sterols. Therefore, FPS may directly increase levels of cholesterol and sterols. Consistently, *S. baumii* triterpenoid content and *FPS* transcription levels are known to fluctuate during different stages [43].

Previous triterpenoid studies have focussed on extraction and purification processes, but the relationship between triterpenoid content and expression levels of key genes has not been fully explored. There may be a delay between changing triterpenoid content and *FPS* expression levels. Studies such as this may provide useful information for investigating *FPS* gene function and ultimately for improving triterpenoid production.

Herein, the *S. baumii FPS*-cDNA, DNA, and promoter regions were cloned for the first time, and analysed by bioinformatics. The expression level of *FPS* and the *S. baumii* triterpenoid content were then explored during different developmental stages, and recombinant FPS was produced in *E. coli* BL21. This type of analysis has not been carried out before, and the results may provide insight into the MVA pathway in *S. baumii*, and knowledge that may

be applicable to other medical fungi. However, methods other than bioinformatics and prokaryotic expression are needed to more fully explore gene function. To this end, we are currently establishing an *Agrobacterium*-mediated transformation system for overexpression and inhibition of *FPS* in future studies.

Acknowledgements This research was supported by the Fundamental Research Funds for the Central Universities, China (2572017CF01).

Compliance with Ethical Standards

Conflict of interest We declare no conflict of interest.

References

1. Zhou, L.-W., Vlasak, J., Decock, C., Assefa, A., Stenlid, J., Abate, D., et al. (2015). 第十二届海峡两岸真菌学学术研讨会大会手册壁报论文摘要集 (Global diversity and taxonomy of the *Inonotus linteus* complex (Hymenochaetales, Basidiomycota): *Sanghuangporus* gen.nov. Tropicoporus excentrodendri and T guanacastensis gen.et spp.nov. and 17 new combinations). *Fungal Diversity* 77(1), 335–347.
2. Sun, J., Chen, Q. J., Zhu, M. J., Wang, H. X., & Zhang, G. Q. (2014). An extracellular laccase with antiproliferative activity from the sanghuang mushroom *Inonotus baumii*. *Journal of Molecular Catalysis B, 99*, 20–25.
3. Wang, F. F., Shi, C., Yang, Y., et al. (2018). Medicinal mushroom*Phellinus igniarius* induced cell apoptosis in gastric cancer SGC-7901 through a mitochondria-dependent pathway. *Biomedicine & Pharmacotherapy, 102*, 18–25.
4. Ge, Q., Mao, J. W., Zhang, A. Q., Wang, Y. J., & Sun, P. L. (2013). Purification, chemical characterization, and antioxidant activity of a polysaccharide from the fruiting bodies of sanghuang mushroom (*Phellinus baumii* Pilát). *Food Science and Biotechnology, 22*(2), 301–307.
5. Taddesse, Y., Lee, W. M., Ko, D., Park, S. C., Cho, J. Y., Park, H. J., et al. (2013). *Phellinus baumii* ethyl acetate extract alleviated collagen type II induced arthritis in DBA/1 mice. *Journal of Natural Medicines, 67*(4), 807–813.
6. Wu, N. (2013). 桑黄子实体中抗衰老化合物的筛选及作用机制的初步探究*(Screening the anti-aging active Components from the fruit of Phellinusbaumii and study on the mechanism of active compounds)*. Shanghai: Shanghai Normal University, PhD. Chinese.
7. Kim, D. I., Kim, K. S., Kang, J. H., & Kim, H. J. (2013). Effect of *Phellinus baumii*-biotransformed soybean powder on lipid metabolism in rats. *Preventive Nutrition and Food Science, 18*(2), 98–103.
8. Xue, Q., Sun, J., Zhao, M. W., Zhang, K., & Lai, R. (2011). Immunostimulatory and anti-tumor activity of a water-soluble polysaccharide from *Phellinus baumii* mycelia. *World Journal of Microbiology and Biotechnology, 27*(5), 1017–1023.
9. Wang, Y. Y., Ma, H., Ding, Z. C., Yang, Y., Wang, W. H., Zhang, H. N., et al. (2019). *baumii*. *International Journal of Biological Macromolecules, 123*, 201–209.
10. Taji, S., Yamada, T., Wada, S., Tokuda, H., Sakuma, K., & Tanaka, R. (2008). Lanostane-type triterpenoids from the sclerotia of *Inonotus obliquus* possessing anti-tumor promoting activity. *European Journal of Medicinal Chemistry, 43*(11), 2373–2379.
11. Zhang, L. F., Sun, T. T., & Zou, L. (2015). 鲍姆纤孔菌总三萜的提取及其体外抗乳腺癌细胞 (MCF-7)活性 (Extraction of total triterpenoids from *Inonotus baumii* and its inhibitory activity on breast cancer cells (MCF-7) in vitro). *Drug Evaluation Research, 38*(5), 497–502.
12. Zhang, G. L., Si, J., Tian, X. M., & Wang, J.-P. (2017). 真菌激发子对桑黄胞内代谢产物积累的影响 (The effects of fungal elicitor on the accumulation of *Sanghuangporus sanghuang* intracellular metabolites). *Mycosystema, 36*(4), 482–491.
13. Sun, T. T., Zou, L., Zhang, L. F., Zhang, J., & Wang, X. (2017). Methyl jasmonate induces triterpenoid biosynthesis in *Inonotus baumii*. *Biotechnology & Biotechnological Equipment, 31*(2), 312–317.
14. Hemmerlin, A., Rivera, S. B., Erickson, H. K., & Poulter, C. D. (2003) Enzymes encoded by the farnesyl diphosphate synthase genefamily in the big sagebrush *Artemisia tridentata* ssp. spiciformis. *Journal of Biological Chemistry,* 278(34), 32132–32140.
15. Rodríguez-Concepción, M., & Boronat A. (2002). Elucidation of the methylerythritol phosphate pathway for isoprenoid biosynthesis in bacteria and plastids. A metabolic milestone achieved through genomics. *Plant physiology*, 130(3), 1079–1089.
16. Hunter, W. N. (2007). The non-mevalonate pathway of isoprenoid precursor biosynthesis. *The Journal of Biological Chemistry, 282*(30), 21573–21577.
17. Liao, Z. H., Chen, M., Gong, Y. F., Li, Z. G., Zuo, K. J., Wang, P., et al. (2006). A new farnesyl diphosphate synthase gene from *Taxus* media rehder: Cloning, characterization and functional. *Journal of Integrative Plant Biology, 48*(6), 692–699.
18. Zjawiony, J. K. (2004). Biologically active compounds from Aphyllophorales (polypore) fungi. *Journal of Natural Products, 67*(2), 300–310.
19. Lange, B. M., Rujan, T., Martin, W., & Croteau, R. (2000). Isoprenoid biosynthesis: the evolution of two ancient and distinct pathways across genomes. *Proceedings of the National Academy of Sciences of the United States of America, 97*(24), 13172–13177.
20. Poulter, C. D. (2006). Farnesyl diphosphate synthase. A paradigm for understanding structure and function relationships in E-polyprenyl diphosphate synthases. *Phytochemistry Reviews*, 5 (1), 17–26.
21. Chen, D. H., Ye, H. C., & Li, G. F. (2000). Expression of a chimeric farnesyl diphosphate synthase gene in *Artemisia annua* L. transgenic plants via Agrobacterium tumefaciens-mediated transformation. *Plant Science, 155*, 179–185.
22. Liu, M. J., Yu, Y. L., Jiang, S., et al. (2018). 珠子参中法尼基焦磷酸合酶(FPS)对皂苷生物合成的影响研究 (Effect of Farnesyl-pyrophosphate Synthase(FPS) on the Biosynthesis of Saponins in *Panax japonicas*). *Bulletin of Botanical Research, 38*(4), 611–618.
23. Fei, Y., Li, N., Zhang, D. H., & Xu, J. W. (2019). Increased production of ganoderic acids by overexpression of homologous farnesyl diphosphate synthase and kinetic modeling of ganoderic acid production in *Ganoderma lucidum*. *Microbial Cell Factories, 18*, 115.
24. Park, H. W., Kim, O. T., Hyun, D. Y., Kim, T. B., Kim, J. U., Kim, Y., et al. (2013). Overexpression of farnesyl diphosphate synthase by introducing cafps gene in *Panax ginseng* C. A. mey. *Korean Journal of Medicinal Crop Science*, 21(1), 32–38.
25. Gupta, P., Akhtar, N., Tewari, S. K., Sangwan, R. S., & Trivedi, P. K. (2011). Differential expression of farnesyl diphosphate synthase gene from with ania somniferain different chemotypes and in response to elicitors. *Plant Growth Regulation, 65*(1), 93–100.

26. Ding, Y. X., -Yang, X., Shang, C. H., Ren, A., Shi, L., Li, Y. X., et al. (2008). Molecular cloning, characterization, and differential expression of a farnesyl-diphosphate synthase gene from the basidiomycetous fungus *Ganoderma lucidum* . *Journal of the Agricultural, 72*(6), 9.
27. Qi, Y., Liu, C., Sun, X., Qiu, L., & Shen J. (2017). The identification of transcriptional regulation related gene of laccase poxc through yeast one-hybrid screeningfrom *Pleurotus ostreatus*. *Fungal Biology* 2017, 121(11), 905–910.
28. Zhang, W. B., Wang, J. G., Li, Z. K., Yang, L. Q., Qin, J., Xiang, Z. H., et al. (2014). 药用真菌桑黄的研究进展 (Progress of studies on medicinal fungus *Phellinus*). *China Journal of Chinese Materia Medica, 39*(15), 2838–2845.
29. Jia, L. (2016). 茯苓总三萜免疫抑制及诱导人结肠癌*RKO*细胞凋亡的研究 *(Study of immunosuppressive activity and apoptosis-inducing effect of total triterpenoids from Poria cocos on human colorectal carcinoma)*. Guangdong: Southern Medical University, PhD. Chinese.
30. Guruprasad, K., Reddy, B. V., & Pandit, M. W. (1990). Correlation between stability of a protein and its dipeptide composition: A novel approach for predicting in vivo stability of a protein from its primary sequence. *Protein Engineering, Design and Selection, 4*(2), 155–161.
31. Garnier, B. J., Gibrat, J. F., & Robson, B. (1996). GOR secondary structure prediction method version IV. *Methods in Enzymology, 266*, 540–553.
32. Waterhouse, A., Bertoni, M., Bienert, S., Studer, G., Tauriello, G., Gumienny, R., et al. (2018). SWISS-MODEL: Homology modelling of protein structures and complexes. *Nucleic Acids Research, 46*(1), 296–303.
33. Guex, N., Peitsch, M. C., & Schwede, T. (2010). Automated comparative protein structure modeling with SWISS-MODEL and Swiss-PdbViewer: A historical perspective. *Electrophoresis, 30*(S1), S162–S173.
34. Bienert, S., Waterhouse, A., & de Beer, T. A. P. (2017). The SWISS-MODEL Repository—new features and functionality. *Nucleic Acids Research, 45*(1), D313–D319.
35. Benkert, P., Biasini, M., & Schwede, T. (2011). Toward the estimation of the absolute quality of individual protein structure models. *Bioinformatics, 27*(3), 343–350.
36. Bertoni, M., Kiefer, F., Biasini, M., Bordoli, L., & Schwede, T. (2017). Modeling protein quaternary structure of homo- and hetero-oligomers beyond binary interactions by homology. *Scientific Reports, 7*(1), 10480.
37. Tachibana, A ., Yano, Y., Otani, S., Nomura, N., Sako Y., & Taniguchi, M. (2000). Novel prenyltransferase gene encoding farnesylgeranyl diphosphate synthase from a hyperthermophilic archaeon, *Aeropyrum pernix*. Molecularevolution with alteration in product *specificity*. *European Journal of Biochemistry*, 267(2), 321.
38. Anderson, M. S., Yarger, J. G., Burck, C. L., & Poulter C. D. (1989). Farnesyl diphosphate synthetase. Molecular cloning, sequence, and expression of an essential gene from *Saccharomyces cerevisiae*. *Journal of Biological Chemistry*, 264(32), 19176–19184.
39. Hemmerlin, A., Rivera, S. B., Erickson, H. K., & Poulter C. D. (2003). Enzymes encoded by the farnesyl diphosphate synthase gene family in the big *Sagebrush Artemisia tridentata* ssp. spiciformis. *Journal of Biological Chemistry*, 278(34), 32132–32140.
40. Cervantes-Cervantes, M. (2006). Maize cDNAs expressed in endosperm encode functional farnesyl diphosphate synthase with geranylgeranyl diphosphate synthase activity. *Plant Physiology, 141*(1), 220–231.
41. Ding, Y. X. (2013). 灵芝法尼基焦磷酸合酶基因的克隆和表达特性研究 (Molecular cloning, characterization, and differential expression of a farnesyl-diphosphate synthase gene from the basidiomycetous fungus *Ganoderma lucidum*). *Nanjing: Nanjing Agricultural University*. PhD Dissertations. Chinese.
42. Zhu, D. Q. (2016). 基因表达过程中涨落与延迟作用机制的研究 *(The study of fluctuation and delay effects in gene expression process), Anhui: University of Science and Technology of China*. Chinese: PhD.
43. Zhang, C. B., Sun, H. X., & Gong, Z. J. (2000). 植物萜类化合物的天然合成途径及其相关合酶 (Plant terpenoid natural metabolism pathways and their synthases). *Plant Physiology Journal, 43*(04), 779–786.